Infrared and Raman Spectroscopic Features of the Self-Interstitial Defect in Diamond from Exact-Exchange Hybrid DFT Calculations
Supplementary Information

Simone Salustro,[1] Alessandro Erba,[1] Claudio M. Zicovich-Wilson,[2] Yves Nöel,[3] Lorenzo Maschio,[1] and Roberto Dovesi[1]

[1] *Dipartimento di Chimica, Università di Torino and NIS - Nanostructured Interfaces and Surfaces - Centre of Excellence, Via Giuria 5, 10125 Torino, Italy*
[2] *Centro de Investigación en Ciencias-(IICBA), Universidad Autónoma del Estado de Morelos, Av. Universidad, 1001, Col. Chamilpa, 62209 Cuernavaca, Morelos (Mexico)*
[3] *Institut des Sciences de la Terre de Paris (UMR 7193 UPMC-CNRS), UPMC, Sorbonne Université, Paris, France*

I. SPIN DENSITY MAPS OF THE ⟨100⟩ SELF SPLIT-INTERSTITIAL

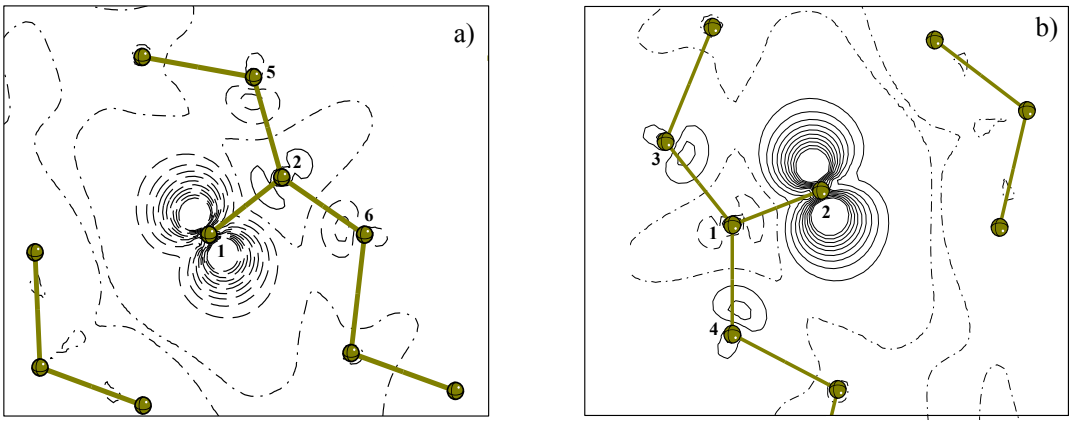

Figure S1: Singlet state spin density maps of the interstitial defective diamond periodic structure along the two planes containing atoms 1, 2, 5 and 6 (a) and 1, 2, 3 and 4 (b). Isodensity lines differ by 0.01 $|e|/(a_0)^3$; spin density truncated at $\pm$ 0.1 $|e|/(a_0)^3$. Continuous, dashed and dot-dashed lines indicate positive, negative and zero values, respectively.

II. EFFECT OF METHODS ON RELATIVE STABILITIES OF SINGLET AND TRIPLET SPIN STATES

Table S1: The ⟨100⟩ split interstitial defect: total energies (in E_h) of S_z=0 (E^0) and S_z=1 (E^1) spin states and their relative stability (ΔE, in mE_h) obtained with several functionals with the S_{33} supercell. The total energy of an S_{32} cell of pristine diamond is -1217.78945 E_h for the B3LYP functional.

Method	E^0	E^1	ΔE
HF	-1248.32495	-1248.32081	4.14
HSE06	-1255.03097	-1255.02970	1.27
PBE0	-1255.05220	-1255.05102	1.18
B3LYP	-1255.46117	-1255.46013	1.04
PBE	-1254.90721	-1254.90625	0.96
LDA	-1245.42792	-1245.42773	0.19

III. EFFECT OF THE SPIN STATE ON WAVENUMBERS

Table S2: Wavenumbers (in cm^{-1}) of the vibrational modes related to the defect for the closed shell, open shell singlet and triplet states. A is the most intense IR active mode. B, C and D are the Raman active modes, which occur at wavenumbers higher than the pristine diamond peak. Labels of the corresponding irreducible representations (IRREP) are also reported.

	Closed			Singlet				Triplet		
Mode	IRREP	S_{33}	S_{65}	IRREP	S_{33}	S_{65}	S_{129}	IRREP	S_{33}	S_{65}
A	E	473.16	510.6	B_2 B_1	495.7 495.7	453.0 452.9	423.2 423.0	E	492.7	450.0
B	B_1	1371.1	1411.3	A_1	1315.9	1340.8	1367.2	B_2	1316.5	1341.3
C	E	1451.6	1489.2	B_2 B_1	1471.6 1473.5	1503.8 1505.7	1529.3 1529.3	E	1477.7	1509.9
D	A_1	1842.8	1901.1	A_1	1837.7	1896.9	1918.9	A_1	1846.3	1905.4

IV. DEFECT CONCENTRATION EFFECT ON BAND STRUCTURES OF THE ⟨100⟩ SELF SPLIT-INTERSTITIAL

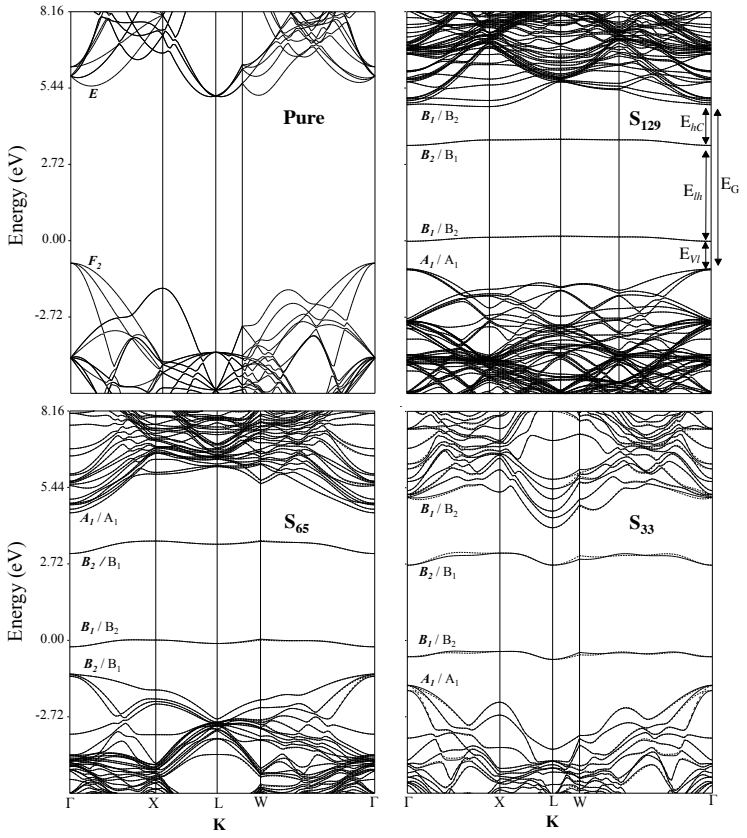

Figure S2: Band structures of pure diamond and of diamond with interstitial defects (S_{129}, S_{65} and S_{33}). Continuous and dashed lines indicate energy levels corresponding to α and β electrons, respectively. Calculations performed with the B3LYP functional. The simmetry of the electronic bands in the gap (evaluated in Γ) are reported for α (**bold**) and β (normal) electrons.

V. POSSIBLE FORMATION OF A DOUBLE BOND IN ⟨100⟩ SELF SPLIT-INTERSTITIAL

In order to better understand the geometrical, electronic and energetic features of the ⟨100⟩ defect, in which the rotation of a couple of atoms (say C_3 and C_4 to give C_3' and C_4', see Figure 1) by 90° is hindered by the covalent network (and by the adopted D_{2d} symmetry), a molecular model with less constraints has been considered: the 2,3-Dimethyl-2-butene (C_6H_{12}), that contains the same backbone of six carbon atoms as in Figure 1, and in which the peripheral C atoms are saturated with 3 H atoms each. The molecule has been investigated at the 90° geometry (with C_{2v} symmetry) as in Figure 1 and in the planar geometry (D_{2h} symmetry); in both cases the symmetry-constrained geometry has been fully optimized; the same functional and basis set have been used as for the bulk. The results are shown in Table S3. The C_1-C_2 distance, that in ⟨100⟩ bulk is only 1.30 Å long, in the 90° rotated molecule is as large as 1.47 Å whereas in the planar molecule is 1.34 Å long. The difference between these two values is a typical difference between a double and a single bond. The short 1.30 Å bond in ⟨100⟩ is then not the evidence of a double bond, rather of a very compressed situation due to the insertion of an additional atom in the very packed structure of diamond. The Overlap Bond Population (OBP) among the two central atoms for the single bond is 0.43 (molecule) and 0.39 $|e|$ (⟨100⟩ interstitial); in the planar molecule, OBP increases to 0.64 $|e|$. The compression in the bulk explains also the short C_1-C_3 distance: 1.42 Å in ⟨100⟩ to be compared to 1.51 Å in the molecule; the spin polarization, on the contrary, on both C_1 and C_3 is essentially the same in the bulk and in the molecule.

The electronic structure and the energy of the two molecular configurations are quite different: the total energy of the planar geometry is 94 mE_h (2.5 eV) lower than that of the "rotated" molecule; moreover, the former is in a singlet state with a double bond and no spin polarization (closed shell, then), the latter a singlet with two unpaired electrons. This suggests that in the ⟨100⟩ split interstitial a rotation of C_3 and C_4 to form a planar local C_6 backbone would bring a consistent energy lowering due to the formation of a double bond. This however would imply to pull the six bonds with the neighbors of C_1 and C_2.

In order to reach additional insight on the possible energy gain and loss with the rotation, and on the related geometry features, our molecular model has been used to investigate also intermediate geometries: a scan of the torsional angle θ from 90° to 0° has been performed allowing relaxation of all other degrees of freedom. In Figure S3 the evolution of the C_1-C_2 distance and OBP, of the total energy of the molecule and of the magnetic moment on the two central atoms is reported. It turns out that, when starting from 90°, the rotation angle must reach about 60° before a sharp modification of all quantities takes place. The C_1-C_2 distance drops down, the OBP increases to values close the the ones typical of a double bond, the atomic magnetic moment μ decreases from one to zero. In summary, a consistent modification of the electronic structure in the interstitial defect of Figure 1 would take place only if the 90° angle would reduce to at least 60°; the cost of this rotation is expected to be larger than the energy gain obtained by the formation of the double bond, as six C-C bonds must be significantly stretched.

This hypothesis has been checked by performing a rigid rotation in the bulk of C_3-C_4 with respect to the C_1-C_2 axis, and of C_5-C_6 in the opposite direction towards the planar configuration. As expected, the energy increases very steeply. When allowed to relax after rotation, by optimizing all parameters in the cell (the rotation reduces the symmetry to D_2), the bulk geometry evolves back to the original 90° configuration. Additional attempts to find a possible lower minimum related to a somehow less orthogonal geometry of the six C atoms, performed eliminating all the symmetry constraints and starting from e deformed geometry, end up in all cases with the 90° geometry. The configuration shown in Figure 1 is by far the most stable with respect to less symmetric situations in which a partial double bond appears.

Table S3: Total energy E (in E_h), interatomic distances R (in Å) and Mulliken analysis data (in |e|) for the C_6H_{12} molecular model; q (net charges), μ (spin momentum) and B (bond population) are reported for two different steric configurations. In D_{2h} the position and the labels of the carbon atoms are as in Figure 1 for the interstitial defect. in C_{2v} the carbon skeleton is planar (3' and 4' white atoms in Figure 1) and there is a double bond among the two central atoms (1 and 2).

Symmetry	E	R(1-2)	R(1-3)	q_1	μ_1	μ_3	B(1-2)
D_{2h}	-235.475	1.345	1.520	-0.054	0.000	0.000	0.636
C_{2v}	-235.381	1.472	1.513	-0.055	1.066	-0.128	0.425

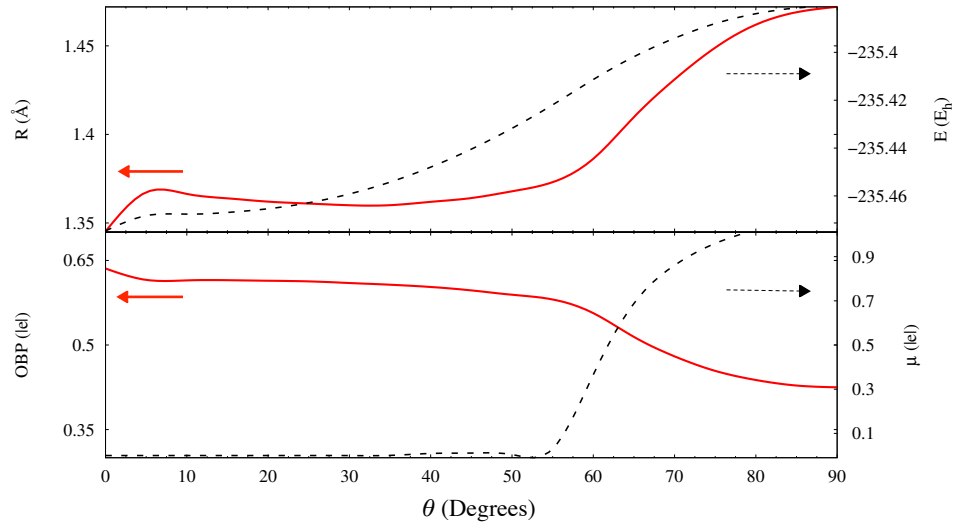

Figure S3: The total energy E, the distance between the two central atoms R, their overlap bond population OBP and the C_1 atomic magnetic moment μ of the C_6H_{12} molecule as a function of the torsional angle θ of the carbon backbone. Continuous lines have the ordinate on the left, dotted lines have the ordinate to the right (see the associated arrows).

VI. ISOTOPIC SUBSTITUTION $^{12}C \rightarrow ^{13}C$ OF THE 6 ATOMS OF THE ⟨100⟩ SELF SPLIT-INTERSTITIAL

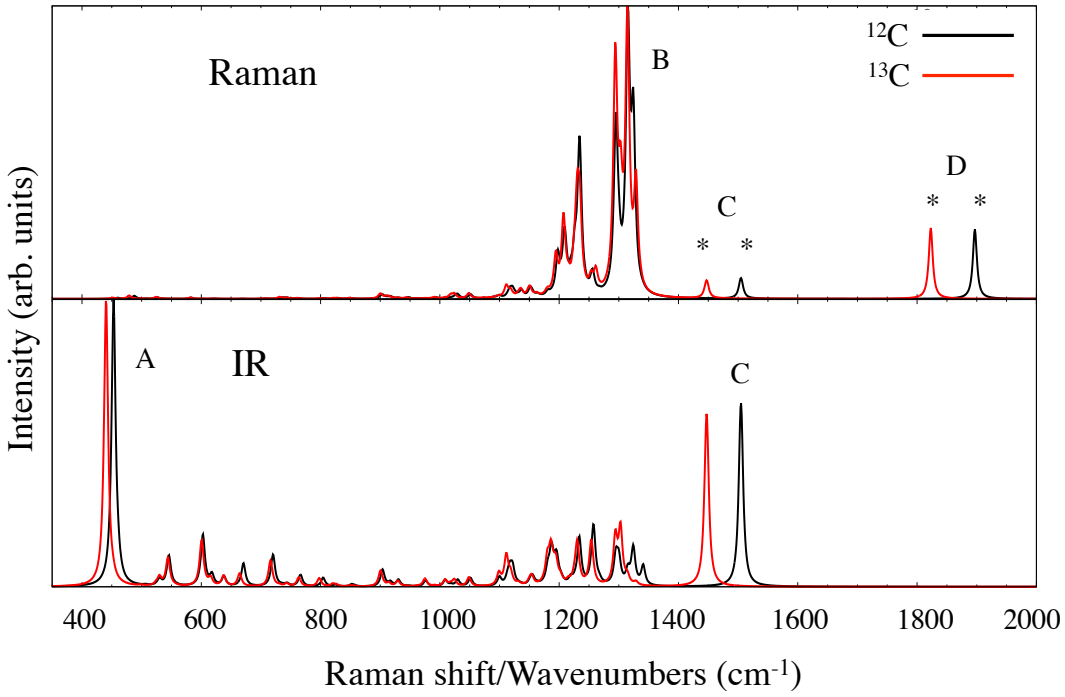

Figure S4: Simulated Raman (upper panel) and IR (lower panel) spectra of ⟨100⟩ defective diamond before (black line) and after (red line) isotopic substitution ($^{12}C \rightarrow ^{13}C$) of the 6 atoms reported in Figure 1 in the article. The intensity of the peaks marked with * has been multiplied by a factor 12. Raman shift variations due to the isotopic substitution for B, C and D peaks are: 1340.2 to 1328.7, 1504.7 to 1447.1, 1896.9 to 1822.9, respectively. IR wavenumber variations for The A peak wavenumber shifts from 453.0 to 440.4.

VII. SPIN DENSITY MAPS AND BAND STRUCTURES FOR THE BOND-CENTERED INTERSTITIAL DEFECT

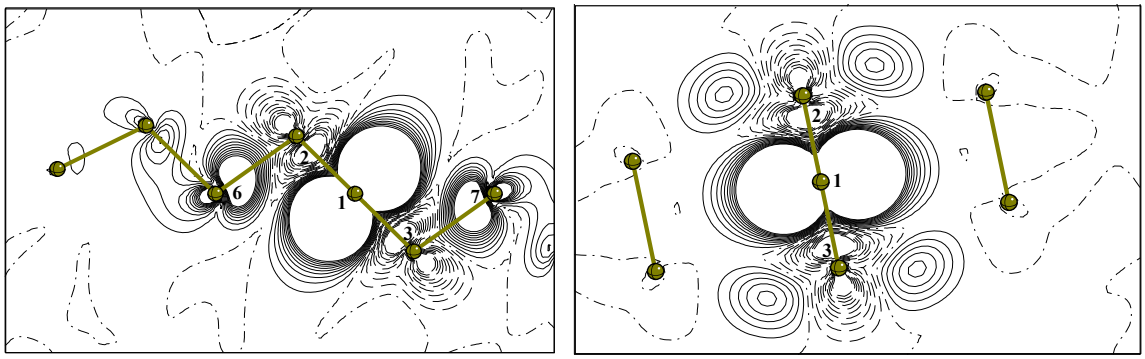

Figure S5: Spin density maps of the BC interstitial defect, for the Sz=1 spin state at the lowest concentration of defects (S_{129}). With reference to Figure 1, in the left panel the spin polarization is projected on the plane containing atoms 1, 2, 3, 6 and 7; in the right panel, spin polarization is projected on the plane orthogonal to the previous one.

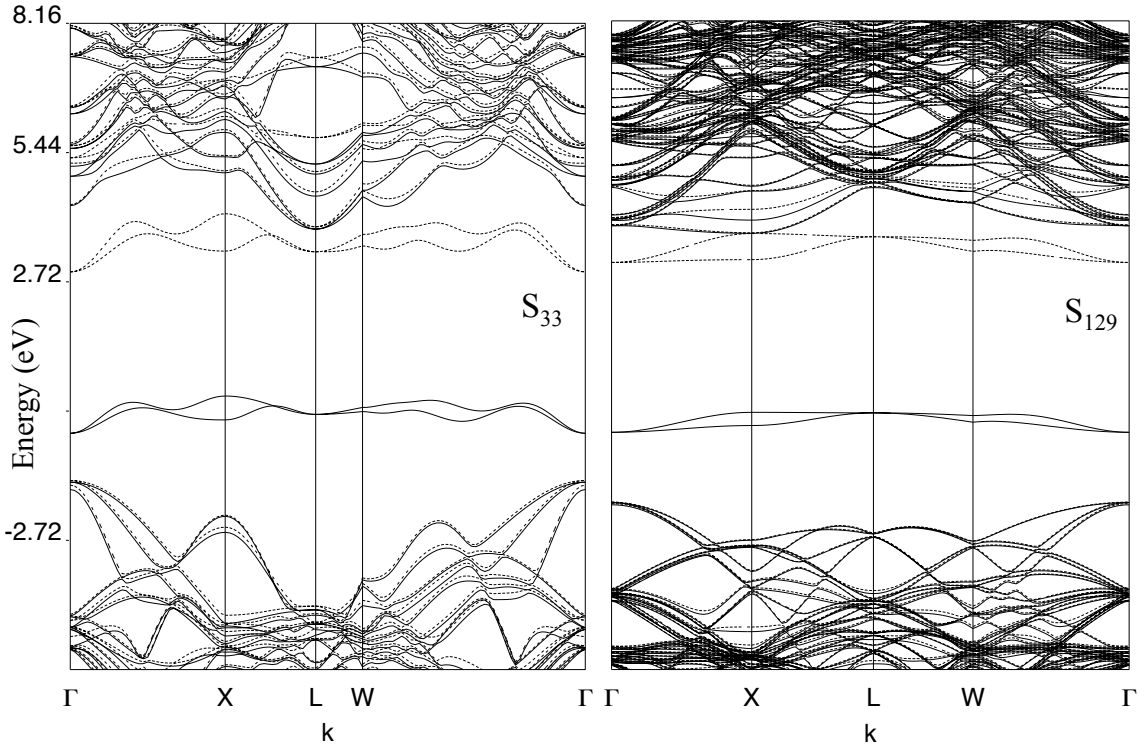

Figure S6: Band structure of the BC interstitial defect, for the S_z=1 spin state at two different concentrations (S_{33} and S_{129}). Continuous and dashed lines indicate energy levels corresponding to α and β electrons, respectively.